

## THE EFFECT OF HEAT INPUT ON THE FRACTURE BEHAVIOUR OF SURFACE WELD METAL OF RAIL STEEL

## UTICAJ UNOSA TOPLOTE NA PONAŠANJE PRI LOMU NAVAREN OG METALA ŠAVA U ČELICIMA ZA ŠINE

Originalni naučni rad / Original scientific paper  
UDK /UDC:

Rad primljen / Paper received: 17.03.2020

Adresa autora / Author's address:

<sup>1</sup>) University of Belgrade, Faculty of Mechanical Engineering, Belgrade, Serbia, email: [opopovic@mas.bg.ac.rs](mailto:opopovic@mas.bg.ac.rs)

<sup>2</sup>) Military Technical Institute, Belgrade, Serbia

<sup>3</sup>) University of Kragujevac, Faculty of Engineering, Kragujevac, Serbia

### Keywords

- heat input
- fracture
- toughness
- crack growth parameters

### Abstract

Surface welding of rail steel with self-shielded wire was conducted with different heat inputs, and the influence of welding heat input on the total impact energy and its components, crack growth rate and fracture mechanism was systematically investigated. It is shown that toughness decreases as heat input increases, but, with a temperature decrease, these differences are not so marked. An increase of heat input leads to increasing the share of transgranular brittle fracture, what is in complete accordance with the obtained energy values. It is established that fatigue life increases when increasing the welding heat input, while resistance to crack growth decreases in the final deposit layer up to the HAZ at all heat inputs. Based on obtained results, the optimal value of heat input is defined for the selected welding procedure.

### INTRODUCTION

Today, rail networks are required to have higher traffic volume with trains traveling at higher speed and heavier axle loads than ever before. The combination of these factors leads to a burden on both railway wheel and rail, which develops damages on contact surfaces /1/. Damaged parts produced from rail high-carbon steel can be surface welded and in spite of their poor weldability this can be an efficient way to prolong their exploitation life. With proper choice of welding technology, it is possible to get a microstructure with improved properties. In that case, the surface welded layer has higher resistance to crack growth, improving overall reliability of rails and crossings, /2/.

Ordinary rail steels contain about 0.5-0.7 wt.% of carbon and are pearlitic. The main properties of these steels are high hardness and strength, and typically low toughness and crack growth resistance. Since they are often exposed to wear and rolling contact fatigue in their exploitation life, parts become unfit for service due to unacceptable profiles, cracking, spalling etc. There has been considerable effort devoted to finding alternatives to the pearlitic rails, but with

### Ključne reči

- unos toplote
- lom
- žilavost
- parametri rasta prsline

### Izvod

Urađeno je navarivanje čelika za šine uz pomoć samozaštitne žice sa različitim unosima toplote, i posmatran je njihov uticaj na ukupnu udarnu energiju i njene komponente, kao i na brzinu rasta prsline i mehanizam loma. Pokazano je da žilavost opada sa povećanjem unosa toplote, ali i da ove razlike nisu toliko izražene u slučaju smanjenja temperature. Povećanje unosa toplote dovelo je do povećanog udela transgranularnog krtog loma, što je u potpunosti u skladu sa dobijenim vrednostima energije. Utvrđeno je da je zamorni vek produžen sa povećanjem unete količine toplote, dok je otpornost prema rastu prsline smanjena u oblasti od poslednjeg sloja prema ZUT, za sve vrednosti unosa toplote. Na osnovu dobijenih rezultata je definisana optimalna količina toplote za konkretni postupak zavarivanja.

varied results. Because bainitic and martensitic steels can be made with higher hardness than pearlite, many studies have examined the wear resistance of these steels. The new generation of bainitic steels achieved higher tensile and fatigue strengths and performed well in service, /3/.

The welding heat input has a great influence on weldment properties. Dependence of mechanical properties on welding conditions has been studied, but the effect of heat input is studied insufficiently, /4/.

At surface welding, heat input affects the mixture ratio, a relevant weld quality parameter. Mixture degree increases with higher heat input, resulting in different microstructures of obtained layers, and in different toughness values. When different welding heat inputs are used, the layers experience different thermal cycles, and different microstructures are formed. Increasing welding heat input restrains the formation of martensite and promotes the transformation of martensite to bainite, /5/.

The most important characteristic of heat input is that it governs the cooling rates in welds, and thereby affects the microstructure of the weld metal. Therefore, the control of

heat input is especially important in arc welding in terms of quality control. The change in toughness is not just tied to the heat input but is also significantly influenced by the weld bead size. As bead size increases, corresponding to a higher heat input, the notch toughness tends to decrease. In multiple-pass welds, a portion of the previous weld pass is refined, and the toughness improved, as the heat from each pass tempers the weld metal underneath. If beads are smaller, more grain refinement occurs, resulting in better notch toughness.

The knowledge of mechanical properties of the weld deposit, especially under dynamic loading is of paramount importance for the quality assessment of welded joints and structures, /6/.

Evaluating fatigue performance, especially fatigue crack growth behaviour of materials and thus, developing a service-life prediction method is a hot issue of structural integrity assessment for structures, /7/. The inhomogeneous microstructure of the dissimilar welded joint is considered as the primary factor resulting in the difference of fatigue crack growth behaviour, /7/. The hardness of the weld metal decreases when increasing welding heat input. As fatigue cracks normally initiate around the bead, a higher hardness of weld metal and HAZ can prevent the initiation of fatigue cracks. Experimental studies have shown that fatigue life is increased when increasing the welding heat input, /8/. Paris pointed out that since the stress intensity factor  $K$  could describe the crack-tip stress field intensity, it could be also considered as the main mechanical parameter controlling the rate of crack growth. Usually, fatigue crack growth can be divided into three regimes: the near-threshold regime, the Paris regime, and the unstable regime. In the near-threshold regime, fatigue crack growth threshold ( $\Delta K_{th}$ ), a crucial parameter for the maximal driving loads permitted for crack non-growth conditions, is influenced by the stress ratio, microstructure, residual stress, and environment, /7/.

## EXPERIMENTAL PROCEDURE

The investigation is carried out with high carbon rail steel, having initial pearlitic microstructure. The chemical composition and mechanical properties are given in Table 1. The surface welding of the test plates is performed with self-shielded wire as filler material (OK Tubrodur 15.43), with chemical composition and mechanical properties given in Table 2. Since the CE-equivalent is 0.64, the calculated preheating temperature is 230 °C, and the controlled inter-pass temperature is 250 °C.

Table 1. Chemical composition and mechanical properties – BM.

Chemical composition, wt. %							$R_m$ (MPa)
C	Si	Mn	P	S	Cu	Al	
0.52	0.39	1.06	0.042	0.038	0.01	0.006	680-830

Table 2. Chemical composition of filler material.

$d$ (mm)	Chemical composition							Hardness HRC
	C	Si	Mn	Cr	Mo	Ni	Al	
1.6	0.15	< 0.5	1.1	1.0	0.5	2.3	1.6	30-40

Surface welding is conducted with three different heat inputs. Welding heat input ( $E$ ) is calculated according to:  $E = 60\eta IU/V$ , where  $I$ ,  $U$ ,  $V$  and  $\eta$  are the welding current,

welding voltage, welding speed and arc efficiency, in respect. Heat input values with welding parameters, are given in Table 3 for 3 samples.

Table 3. Sample designation and welding parameters.

Sample no.	Welding current (A)	Voltage (V)	Welding speed (cm/s)	Heat input (J/cm)
1	180	28	47	6 440
2	235	30	40	10 520
3	280	30	31.8	15 850

Surface welding is performed in three layers (samples 1 and 2), except for sample 3, where the required thickness of the weld (10 mm) is obtained in two layers, due to the high heat input.

Specimens for further investigation are prepared from the weld metal of surface welded samples. Impact testing is performed according to EN 10045-1, i.e. ASTM E23-95, with Charpy specimens, V notched in the WM, using the instrumented machine SCHENCK TREBEL 150 J. Specimens are cut and tested at 20 °C, -20 °C and -40 °C. Then, the fractured surfaces are examined by scanning electron microscope (SEM) Jeol JSM-6610 LV, with electron acceleration voltage of 20 kV and magnification of 1000 $\times$ . Fatigue crack growth tests are performed on CRACK-TRONIC dynamic testing device in the FRACTOMAT system, with standard Charpy specimens at room temperature, under the ratio  $R = 0.1$ . Standard 2 mm V notch is located in the third layer of WM, and the initiated crack was propagated, enabling calculation of crack growth rate  $da/dN$  and fatigue threshold  $\Delta K_{th}$ . Figure 1 shows the location of V notch for fatigue crack growth testing.

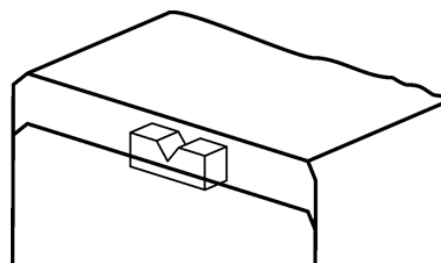


Fig. 1. Location of the V-notch for fatigue crack growth test

## RESULTS AND DISCUSSION

Instrumented Charpy pendulum enables the separation of total impact ( $E_t$ ) to crack initiation ( $E_{in}$ ) and crack propagation energy ( $E_{pr}$ ). Impact testing results at test temperatures for all samples are given in Table 4 and in Fig. 2.

Table 4. Results for Charpy V surface weld metal.

		20 °C	-20 °C	-40 °C
sample 1 6.4 kJ/cm	$E_t$ (J)	32	25	15
	$E_{in}$ (J)	20	19	14
	$E_{pr}$ (J)	12	6	1
sample 2 10.5 kJ/cm	$E_t$ (J)	29	23	17
	$E_{in}$ (J)	20	16	15
	$E_{pr}$ (J)	9	7	2
sample 3 15.9 kJ/cm	$E_t$ (J)	21	18	16
	$E_{in}$ (J)	17	15	13
	$E_{pr}$ (J)	4	3	3

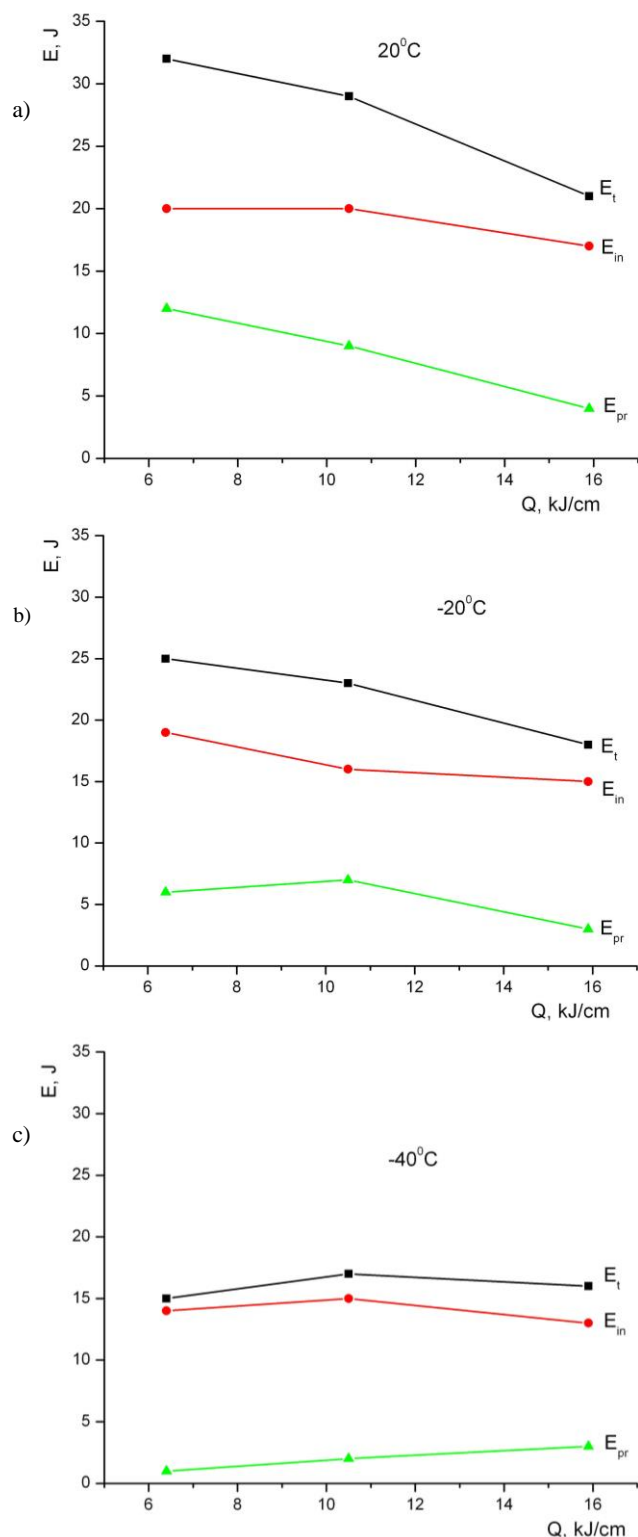


Figure 2. Total energy, crack initiation and crack propagation energy vs. heat input at: a) 20°C; b) -20°C; c) -40°C.

At room temperature, the total impact energy is highest for the lowest heat input (6.4 kJ/cm), and is equal to 32 J. With an increase of heat input, impact energy decreases and is 21 J for 15.9 kJ/cm of heat input. Crack propagation energy,  $E_{pr}$ , is very low (4-12 J) and in all cases is lower than crack initiation energy,  $E_{in}$ , at -20 °C, the lowest total

impact energy is obtained for the highest heat input (18 J), while the highest impact energy is achieved with the sample of lowest heat input (25 J). Crack initiation energy is equal to 15-19 J. At -40 °C, the differences between samples are minimal (15-17 J), and the proportion of crack propagation energy at this temperature is negligible. Due to crack initiation energy being insensitive to temperature decrease, these joints are satisfactory and safe in exploitation up to -40 °C.

By analysing impact energy values of the samples, a change in toughness continuity is observed, with no marked drop in toughness. Since the crack initiation energy is higher than the crack propagation energy at all test temperatures, this is the reason for the absence of significant decrease in toughness.

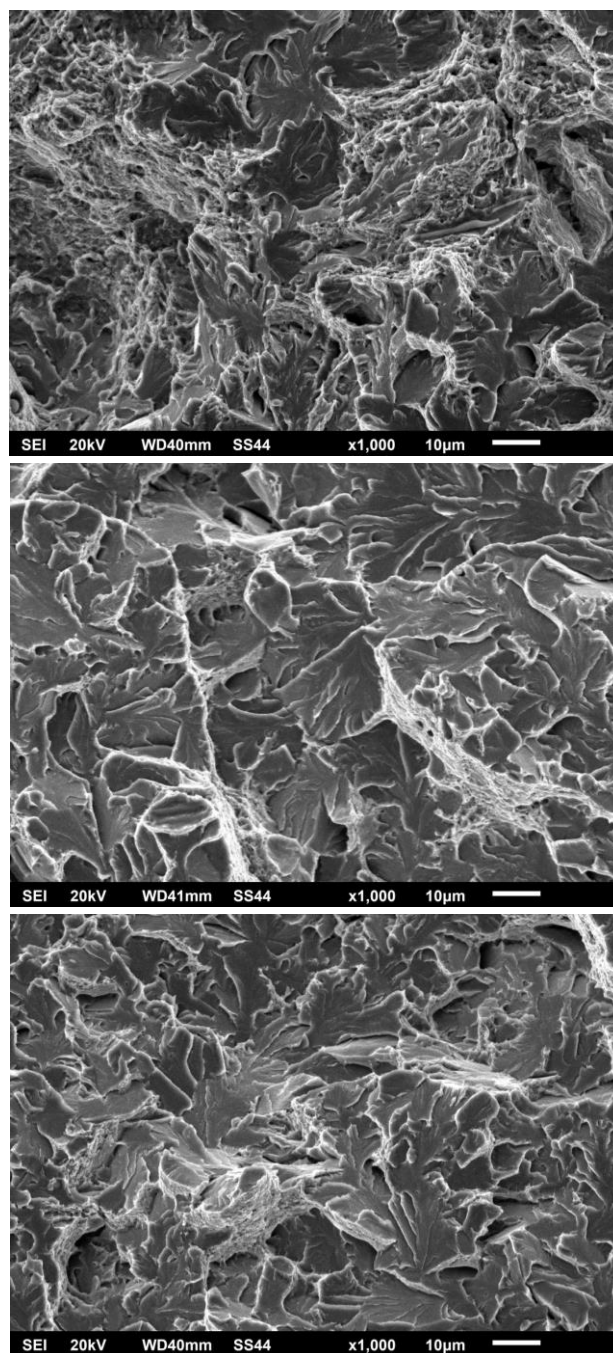


Figure 3. Fractography of Charpy specimens from the central zone.

Fractographic investigation of all three Charpy specimens at room temperature indicates several clearly distinguished zones. In the zone of stable crack growth, located directly below the notch, ductile transgranular fracture is dominant. The size of this zone changes and is the largest in sample 1. At transition to unstable growth, the fracture mechanism changes, so a small amount of brittle transgranular fracture by cleavage in certain planes appears. Furthermore, the proportion of brittle component increases to the final stage of fracture, where transgranular brittle fracture becomes dominant. Figure 3 shows the typical fractography from the central zone of fracture in the three samples. It is noted that an increase in heat input leads to an increase in the portion of transgranular brittle fracture, what is in complete accordance with obtained energy values.

Results of crack growth resistance parameters, i.e., obtained relationship  $da/dN$  vs.  $\Delta K$  for all heat inputs are given in Fig. 4. Parameters  $C$  and  $m$  in Paris law, fatigue threshold  $\Delta K_{th}$  and crack growth rate values are given in Table 5 as obtained from relationships given in Fig. 4, for corresponding  $\Delta K$  values.

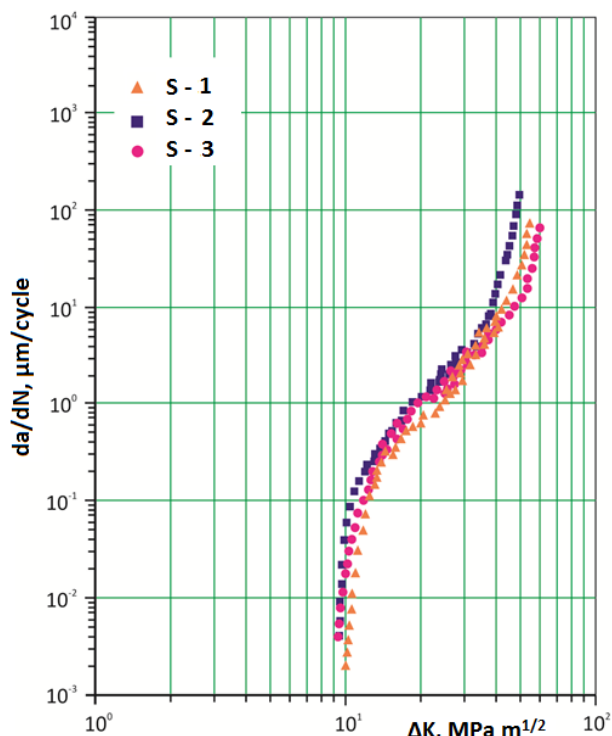


Figure 4.  $da/dN$  vs.  $\Delta K$  for all heat inputs and fracture at room temperature, samples 1-3.

The behaviour of welded joint and its constituents should affect the curve slope in the part of validity of the Paris law. Due to the fact the surface weld layer consists of several layers, parameters  $C$ ,  $m$  and crack growth rate are determined for each layer (Table 5). Since the V notch is located in the third layer of WM, the initiated crack propagates through other two layers into the HAZ. For comparing the properties of the surface welded joint, the crack growth rate is calculated for the same values of stress intensity factor range  $\Delta K$  (20, 25 and 30  $\text{MPa m}^{1/2}$ ). It is important that the selected value is within the middle part of the diagram,

where the Paris law is applied. It is noted that samples 2 and 3 have three times lower crack growth rate compared to sample 1 ( $1.11 \cdot 10^{-8}$  and  $1.01 \cdot 10^{-8}$  compared to  $3.77 \cdot 10^{-8}$   $\text{m/cycle}$ ). This means that for the same value of stress intensity factor  $\Delta K$ , sample 1 needs less cycles of variable amplitude.

Table 5.  $C$ ,  $m$ ,  $\Delta K_{th}$  (in  $\text{MPa m}^{1/2}$ ) and crack growth rates.

sample	zone	$\Delta K_{th}$	$C$	$m$	$da/dN$ (m/cycle)		
					$\Delta K=20$	$\Delta K=25$	$\Delta K=30$
1	WM 1	9.7	$4.04 \cdot 10^{-13}$	3.82	$3.77 \cdot 10^{-8}$	-	-
	WM 2		$3.28 \cdot 10^{-13}$	3.97	-	$1.16 \cdot 10^{-7}$	-
	HAZ		$3.43 \cdot 10^{-13}$	3.88	-	-	$3.36 \cdot 10^{-7}$
2	WM 1	9.5	$4.45 \cdot 10^{-13}$	3.74	$1.11 \cdot 10^{-8}$	-	-
	WM 2		$3.78 \cdot 10^{-13}$	3.61	-	$1.88 \cdot 10^{-8}$	-
	HAZ		$4.07 \cdot 10^{-13}$	3.79	-	-	$1.61 \cdot 10^{-7}$
3	WM 1	9.3	$4.37 \cdot 10^{-13}$	3.71	$1.01 \cdot 10^{-8}$	-	-
	WM 2		$3.62 \cdot 10^{-12}$	3.64	-	$4.44 \cdot 10^{-8}$	-
	HAZ		$4.45 \cdot 10^{-12}$	3.76	-	-	$4.70 \cdot 10^{-7}$

It should also be noted that resistance to crack growth in all samples decreases from the final layer to the HAZ. The maximal fatigue crack growth rate is achieved in HAZ for all samples when stress intensity factor range approaches to plane strain fracture toughness.

If a structural component is continuously exposed to variable loads, fatigue crack may initiate and propagate from severe stress raisers if the stress intensity factor range at fatigue threshold  $\Delta K_{th}$  is exceeded. The fatigue threshold value  $\Delta K_{th}$  is the lowest for sample 3 ( $9.3 \text{ MPa m}^{1/2}$ ), thus the crack in sample 3 will initiate earlier, i.e. after less cycles than in samples 1 and 2.

Values of fatigue threshold and crack growth rates correspond to initiation and propagation energies in impact tests. In the case of the fatigue threshold value and crack initiation energy, good correlation is achieved. Sample 1 has the highest crack initiation energy (20 J) and the highest  $\Delta K_{th} = 9.7 \text{ MPa m}^{1/2}$ . When comparing crack propagation energy and crack growth rate, it is hard to establish the precise analogy, as toughness is estimated for the surface weld metal, whereas the crack growth rate for each surface weld layer.

## CONCLUSIONS

On the basis of obtained experimental results and their analysis, the following is concluded.

Experimental investigation of surface welded joints with different heat inputs has shown, as expected, significant differences on their performance in terms of mechanical properties. The heat input energy is an especially important parameter that affects the microstructure and weld quality.

The experiment is conducted with energies selected on the basis of literature recommendations for welding similar steels. Notwithstanding the significant differences, each of the selected heat inputs provides satisfactory properties and safe exploitation.

Comparing the samples surfaced with different heat inputs, noting that the toughness decreases with heat input increase, and in terms of toughness, optimal heat input is in the lower range of values for applied welding procedure.

But, with a temperature decrease, the differences are lower, and the optimal value of heat input is shifted to higher values. Therefore, it is particularly important to define the working conditions of welded structures.

Values of crack growth rate change with crack propagation through different deposited layers and it is shown that heat input affects these values. Taking into account all the layers, it is noted that the sample welded with the lowest heat input (sample 1) shows the lowest resistance to crack growth, while sample 2 (10.5 kJ/cm) shows the highest resistance. Also, it is shown that resistance to crack growth in all samples decreases from the final deposit layer to HAZ. The fatigue threshold value  $\Delta K_{th}$  is the lowest for sample 3, meaning that the crack in sample 3 will initiate earlier, i.e. after less cycles, than in samples 1 and 2.

Fractographic investigation of Charpy specimens at room temperature shows that in all samples, ductile transgranular fracture is dominant with different amounts of transgranular brittle fracture. An increase of heat input leads to increased share of transgranular brittle fracture, what is in complete accordance with the obtained energy values.

Based on the above, taking into account the toughness at room and low temperatures, resistance to crack growth and fractographic analysis, it can be concluded that the heat input value of about 10 kJ/cm is optimal.

#### ACKNOWLEDGEMENT

The research is performed in the frame of the national project TR 35024 (Contract 451-03-68/2020-14/200105) financed by the Ministry of Education, Science and Technological Development of the Republic of Serbia.

#### REFERENCES

1. Lee, S.-H., Kim, S.H., Chang, Y.-S., Jun, H.K. (2014), *Fatigue life assessment of railway rail subjected to welding residual and contact stresses*, J Mech. Sci. Technol. 28(11): 4483-4491. doi: 10.1007/s12206-014-1016-3
2. Popović, O., Prokić-Cvetković, R., Sedmak, A., et al. (2011), *The influence of buffer layer on the properties of surface welded joint of high-carbon steel*, Materijali in tehnologije 45(6): 579-584.
3. Popović, O., Prokić-Cvetković, R. (2012), *Surface Welding as a Way of Railway Maintenance*, Chapter 10 in Mechanical Engineering, Ed. Murat Gokcek, InTechOpen: 233-253. doi: 10.5772/35403
4. Pirinen, M., Martikainen, Yu., Layus, P.D., et al. (2015), *Effect of heat input on the mechanical properties of welded joints in high-strength steels*, Svarochnoe Proizvodstvo 2015(2): 14-17. doi: 10.1080/09507116.2015.1036531
5. Dong, H., Hao, X., H., Deng, D. (2014), *Effect of welding heat input on microstructure and mechanical properties of HSLA steel joint*, Metallogr. Microstruct. Anal. (2014) 3: 138-146. doi: 10.1007/s13632-014-0130-z
6. Ghosh, P.K., Nagesh Babu, P., Gupta, P.C. (1994), *Microstructure-fatigue crack growth rate correlation in multipass submerged arc C-Mn steel weld deposit*, ISIJ Int. 34(3): 280-284. doi: 10.2355/isijinternational.34.280
7. Deng, X., Lu, F., Cui, H., et al. (2016), *Microstructure correlation and fatigue crack growth behavior in dissimilar 9Cr/CrMoV welded joint*, Mater. Sci. & Eng. A 651: 1018-1030. doi: 10.1016/j.msea.2015.11.081
8. Suh, C.H., Lee, R.G., Oh, S.K., et al. (2011), *Effect of welding heat input on fatigue life of quenched boron steel and FB steel lap joint*, J Mech. Sci. Technol. 25(7): 1727-1735. doi: 10.1007/s12206-011-0424-x

© 2020 The Author. Structural Integrity and Life, Published by DIVK (The Society for Structural Integrity and Life 'Prof. Dr Stojan Sedmak') (<http://divk.inovacionicentar.rs/ivk/home.html>). This is an open access article distributed under the terms and conditions of the [Creative Commons Attribution-NonCommercial-NoDerivatives 4.0 International License](#)

